Supplementary information to:

Bacterial actin MreB assembles in complex with cell shape protein RodZ

by

Fusinita van den Ent[&], Christopher M. Johnson[§], Logan Persons[#], Piet de Boer[#] and Jan Löwe[&]

[&] MRC Laboratory of Molecular Biology, Hills Road Cambridge CB2 0QH, UK

[§] MRC Centre for Protein Engineering, Hills Road Cambridge CB2 0QH, UK

[#] Dept of Molecular Biology and Microbiology, Case Western Reserve University, Cleveland OH 44106, USA

A

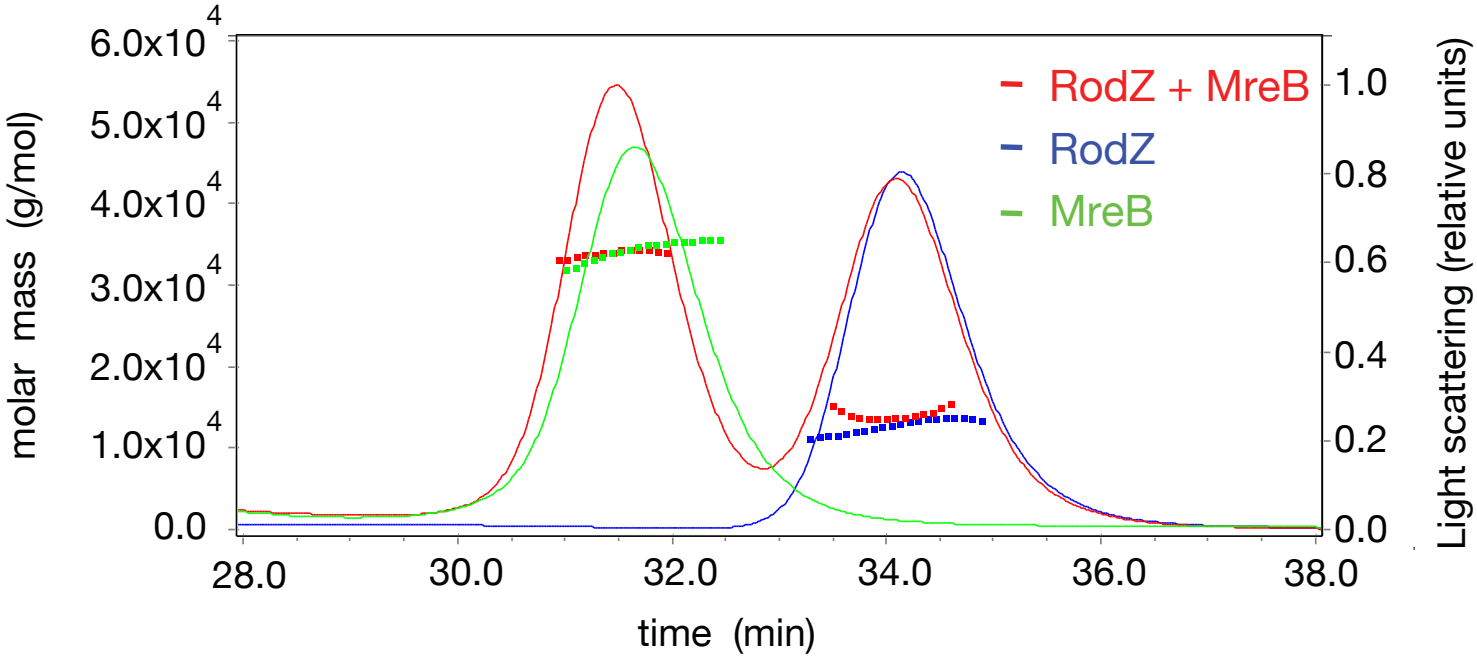
molar mass (g/mol)
6.0x10^4
5.0x10^4
4.0x10^4
3.0x10^4
2.0x10^4
1.0x10^4
0.0
28.0
30.0
32.0
34.0
36.0
38.0
time (min)
RodZ + MreB
RodZ
MreB
Light scattering (relative units)
1.0
0.8
0.6
0.4
0.2
0.0

B

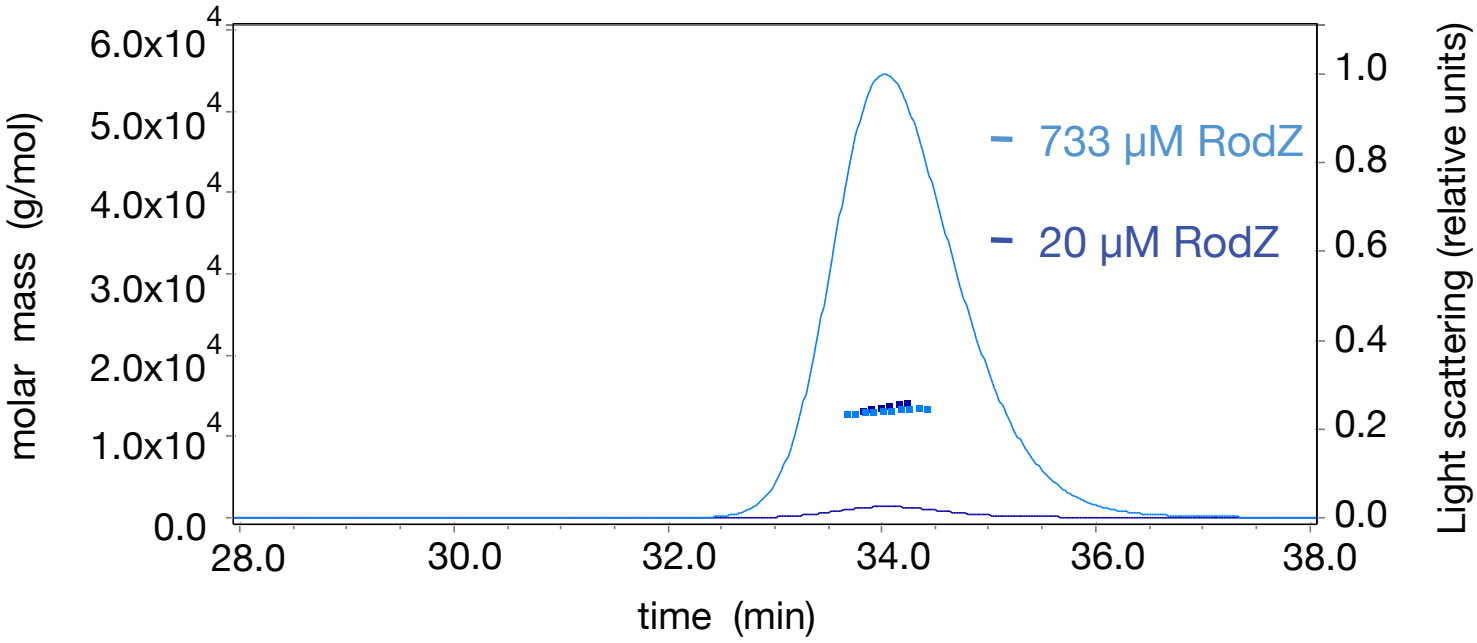
molar mass (g/mol)
6.0x10^4
5.0x10^4
4.0x10^4
3.0x10^4
2.0x10^4
1.0x10^4
0.0
28.0
30.0
32.0
34.0
36.0
38.0
time (min)
733 µM RodZ
20 µM RodZ
Light scattering (relative units)
1.0
0.8
0.6
0.4
0.2
0.0

Fig S1

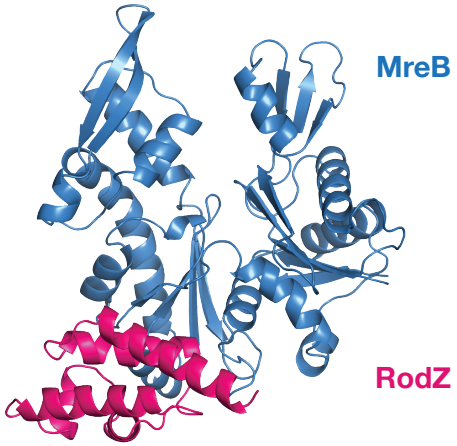
MreB
RodZ

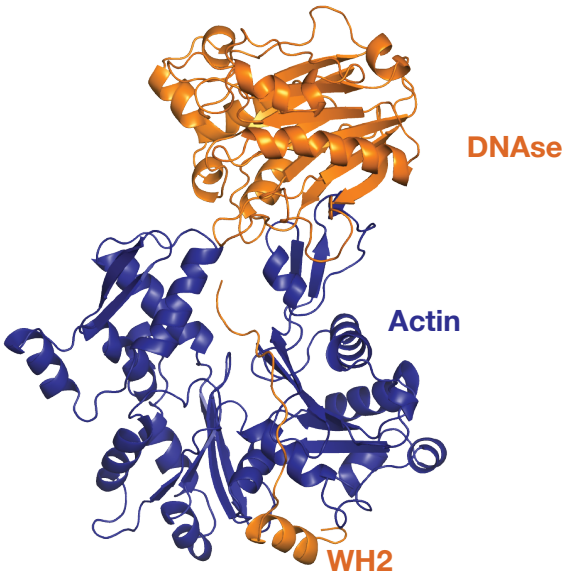
DNAse
Actin
WH2

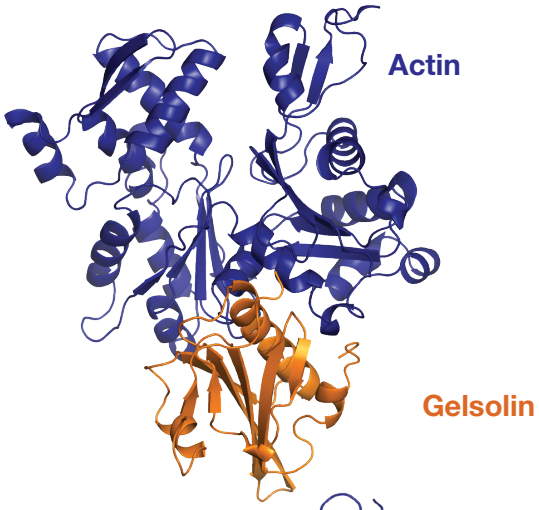
Actin
Gelsolin

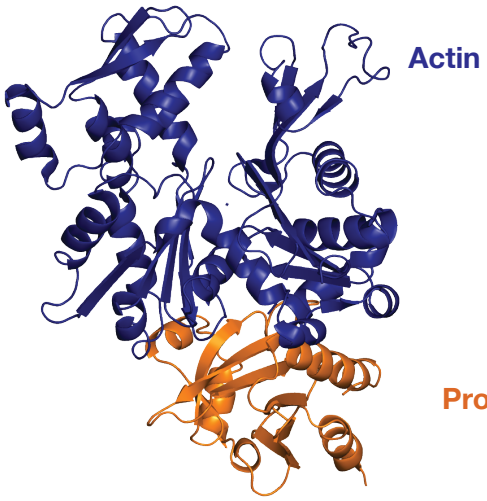
Actin
Profilin

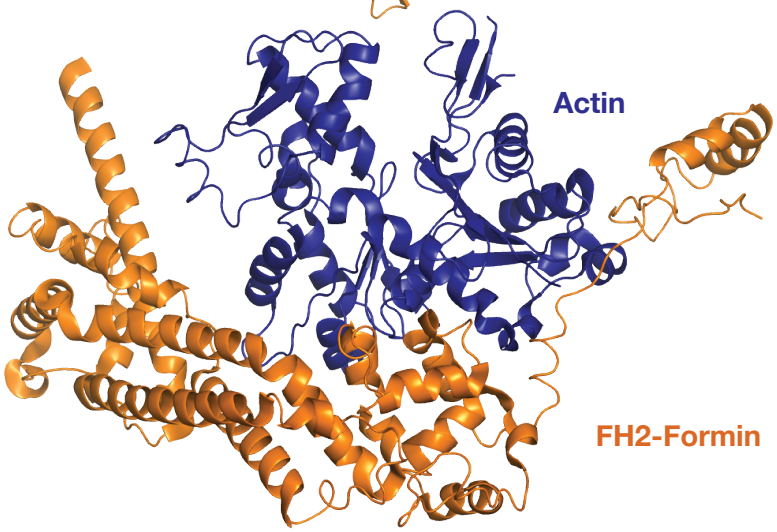
Actin
FH2-Formin

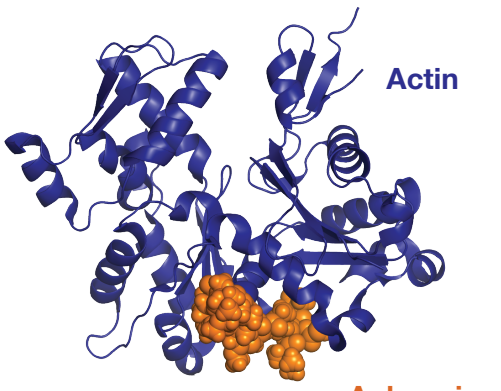
Actin
Aplyronine

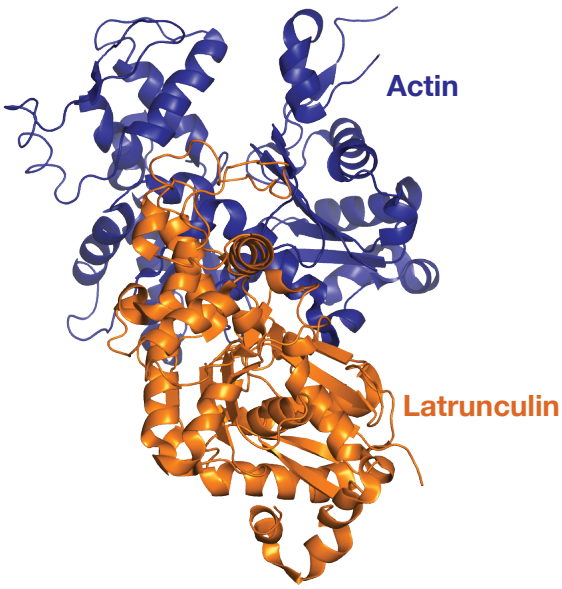
Actin
Latrunculin

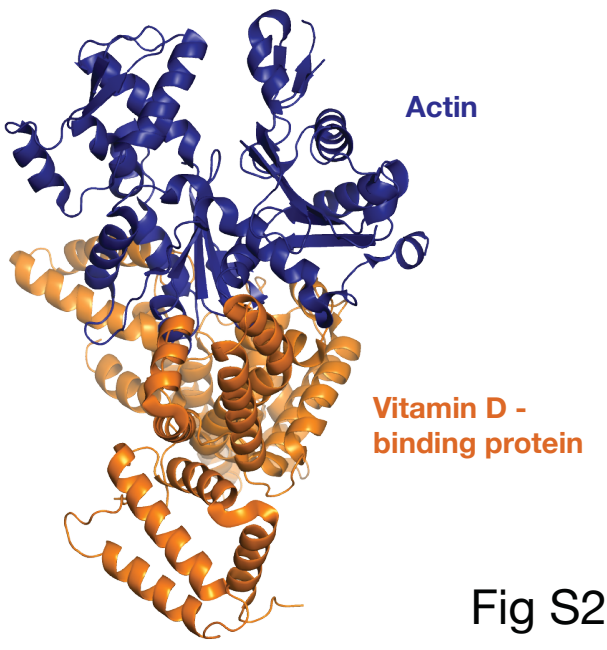
Actin
Vitamin D -
binding protein

Fig S2

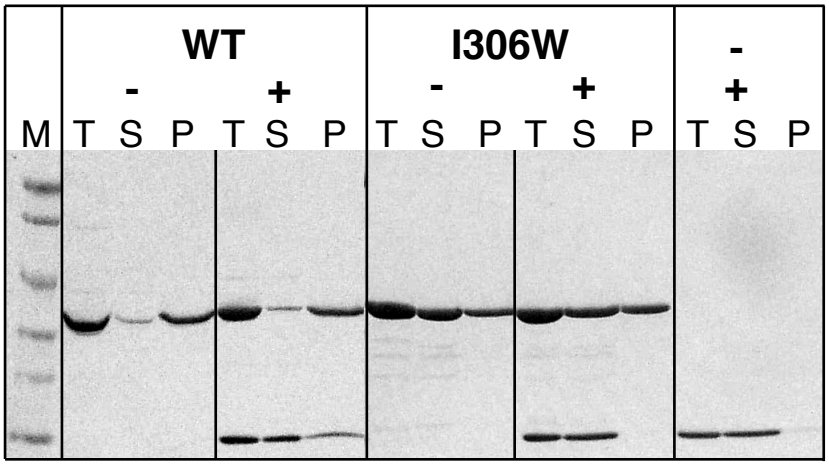

Fig. S3

Fig S1. Size-exclusion chromatography - multi angle light scattering (SEC-MALS). A. Protein samples used for ITC measurements were analysed using SEC-MALS: MreB (24 μM, in green) and $RodZ^{(1-104)}$ (140 μM, in blue). The evaluated mass is correct for the monomer and the distribution of mass across the peak is constant, indicating a single monodisperse species for both MreB and $RodZ^{(1-104)}$. Following ITC, the sample, analysed by SEC-MALS shows slightly shifted peaks compared to the proteins alone (MreB 26 μM, RodZ 140 μM, red trace). The samples were separated on a Superdex S200 in 20 mM Tris-HCl, pH 7.5, 1 mM EDTA, 1 mM Sodium azide, 200 mM NaCl and analysed using MALS. **B.** $RodZ^{(1-104)}$ examined over a wide concentration range (as indicated in the figure) is shown to be monomeric by SEC-MALS in 20 mM Tris-HCl, pH 7.5, 1 mM EDTA, 1 mM Sodium azide, 200 mM NaCl.

Fig S2. Comparison of bacterial and eukaryotic actin complexes. Ribbon plot of bacterial actin homologue MreB (sky blue) in complex with the cytoplasmic domain of RodZ (magenta) from *T. maritima*, compared to heterodimers of actin (dark blue) in complex with its binding partners (orange). PDB entry code for actin complexes are: 2D1K for actin-DNAse, 1YAG for actin-gelsolin, 2BTF for actin-profilin, 1Y64 for actin-FH2-formin, 1WUA for actin-aplyronine, 1IJJ for actin-latrunculin, 1KXP for actin-vitamin D-binding protein.

Fig S3. MreB polymerisation assays were used to test the interface mutants of MreB for RodZ binding. MreB (28 μM) was incubated in the presence and absence of $RodZ^{(1-104)}$ (35 μM) with nucleotide and $MgCl_2$ at 37°C. The pellet was separated from the supernatant by centrifugation at 140,000g. Total (T), supernatant (S) and pellet (P) was analysed on a 10-20% gradient gel and stained with Coomassie. Mutations in MreB are shown above the panels. Protein marker (M) depicts molecular weights of 113, 92, 53, 35, 39 and 22 kDa.

Role of helix-turn-helix motif in RodZ. The movie shows a classical HTH motif (pdb entry 2or1, rainbow colored with N-terminus in blue) in complex with double stranded DNA (grey). The first three α-helices of RodZ are superimposed on to the classical HTH motif, showing the degree of conservation (red conserved, white average, green variable). A highly conserved area emerges when turning the HTH motif around that accommodates the 4^{th} helix of RodZ. The major interface between RodZ and MreB is formed by helix 4. Tyr 53 (depicted as spheres) is part of this helix and fits into a hydrophobic and reasonable conserved pocket of MreB.

Table II: *E.coli* plasmids used in the *in vivo* work.

Plasmid	Relevant genotype [a]	ori	Source or Reference
pCH375	*aph* P_{lac}::*mreB'-t25-'mreB*	pACYC	(Bendezú et al., 2009)
pCH395	*bla lacI*^{q} P_{lac}::*t18-rodZ*(1-138)-*rfp*	ColE1	This work
pCH395 (D55A)	*bla lacI*^{q} P_{lac}::*t18-rodZ*(1-138, D55A)-*rfp*	ColE1	This work
pCH395 (L56G)	*bla lacI*^{q} P_{lac}::*t18-rodZ*(1-138, L56G)-*rfp*	ColE1	This work
pCH395 (F60A)	*bla lacI*^{q} P_{lac}::*t18-rodZ*(1-138, F60A)-*rfp*	ColE1	This work
pCH395 (Y64A)	*bla lacI*^{q} P_{lac}::*t18-rodZ*(1-138, Y64A)-*rfp*	ColE1	This work
pCH395 (R66A)	*bla lacI*^{q} P_{lac}::*t18-rodZ*(1-138, R66A)-*rfp*	ColE1	This work
pCH395 (S67A)	*bla lacI*^{q} P_{lac}::*t18-rodZ*(1-138, S67A)-*rfp*	ColE1	This work
pFB273	*att*HK022 *bla lacI*^{q} P_{lac}::*gfp-t-rodZ*	R6K	(Bendezú et al., 2009)
pFB273 (D55A)	*att*HK022 *bla lacI*^{q} P_{lac}::*gfp-t-rodZ*(D55A)	R6K	This work
pFB273 (L56A)	*att*HK022 *bla lacI*^{q} P_{lac}::*gfp-t-rodZ*(L56G)	R6K	This work
pFB273 (F60A)	*att*HK022 *bla lacI*^{q} P_{lac}::*gfp-t-rodZ*(F60A)	R6K	This work
pFB273 (Y64A)	*att*HK022 *bla lacI*^{q} P_{lac}::*gfp-t-rodZ*(Y64A)	R6K	This work
pFB273 (R66A)	*att*HK022 *bla lacI*^{q} P_{lac}::*gfp-t-rodZ*(R66A)	R6K	This work
pFB273 (S67A)	*att*HK022 *bla lacI*^{q} P_{lac}::*gfp-t-rodZ*(S67A)	R6K	This work
pKNT25	*aph* P_{lac}::*lacZ'-t25*	pACYC	(Karimova et al., 2005)
pLP39	*att*HK022 *bla lacI*^{q} P_{lac}::*gfp-t-rodZ*(1-138)-*rfp*	R6K	This work
pLP39 (D55A)	*att*HK022 *bla lacI*^{q} P_{lac}::*gfp-t-rodZ*(1-138, D55A)-*rfp*	R6K	This work
pLP39 (L56G)	*att*HK022 *bla lacI*^{q} P_{lac}::*gfp-t-rodZ*(1-138, L56G)-*rfp*	R6K	This work
pLP39 (F60A)	*att*HK022 *bla lacI*^{q} P_{lac}::*gfp-t-rodZ*(1-138, F60A)-*rfp*	R6K	This work
pLP39 (Y64A)	*att*HK022 *bla lacI*^{q} P_{lac}::*gfp-t-rodZ*(1-138, Y64A)-*rfp*	R6K	This work
pLP39 (R66A)	*att*HK022 *bla lacI*^{q} P_{lac}::*gfp-t-rodZ*(1-138, R66A)-*rfp*	R6K	This work
pLP39 (S67A)	*att*HK022 *bla lacI*^{q} P_{lac}::*gfp-t-rodZ*(1-138, S67A)-*rfp*	R6K	This work

[a]Genotypes indicate when constructs encode in-frame Gfpmut2 (*gfp*), mCherry (*rfp*), T7.tag, (*t*), CyaA T18-domain (*t18*), or CyaA T25-domain (*t25*) sequences.

Table III: Effects of helix 4 mutations on *in vivo* properties of *E. coli* RodZ

E.c.	T.m.	T18/GFP-RodZ$^{1-138}$-RFP				GFP-RodZ		
		[a]x MreB-T25^{SW}	[b]Localisation		[c]Shape	[b]Localisation		[c]Shape
			TB28 [*wt*]	FB60 [Δ*rodZ*]		TB28 [*wt*]	FB60 [Δ*rodZ*]	
wt	-	+	Sp	Sp	++	Sp	Sp	++
D55A	L48	+	Sp	Sp	++	Sp	Sp	++
L56G	D49	+	Sp	Sp	++	Sp	Sp	++
F60A	Y53	-	M	M	-	M+Sp	M+Sp	+
Y64A	Y57	-	M	M	-	M+Sp	M+Sp	+
R66A	K59	+	Sp	Sp	++	Sp	Sp	++
S67A	R60	+	Sp	Sp	++	Sp	Sp	++

[a]Results from BACTH assays. +, interaction of T18-RodZ$^{1-138}$-RFP with MreB-T25^{SW}; -, no interaction.

[b]Localisation of GFP-RodZ-RFP and GFP-RodZ$^{1-138}$-RFP fusions in wt and Δ*rodZ* cells. M, evenly along membrane; Sp, spiral-like/spotty along membrane; M+Sp, mostly evenly along membrane plus some associated spots of higher intensity.

[b]Correction of rod-shape by GFP-RodZ-RFP and GFP-RodZ$^{1-138}$-RFP fusions in Δ*rodZ* cells. ++, full correction (> 99% rod-shaped, resembles wildtype); +, partial correction (~75% rod-like, though most cells wider than normal, and the rest a mix of spheroids, lemons, branched, and other atypical shapes); -, no correction (> 99% spheroid).

Materials and methods

***E. coli* plasmids**

Relevant plasmids are listed in Table II (supplementary information). Plasmids pDR120 (Hale and de Boer, 1999), and pCH371, pCH393, pFB233, pFB249, pTB183, and pYT27 (Bendezú et al., 2009) have been described before.

To obtain pCH395 [P_{lac}::*t18-rodZ*(1-138)-*rfp*], a portion of pFB249 [P_{lac}::*rodZ*(1-138)-*rfp*] was amplified with primers 5'-GTACTCTAGAGGCCATTACGGCCATGAATACTGAAGCC-3' and 5'-AGCTGGCCGAGGCGGCCTTATTTGTACAGCTCATCCATGC-3'. The product was digested with *Sfi*I (underlined) and the 1153 bp fragment was used to replace the 1027 bp *Sfi*I fragment of pCH371 [P_{lac}::*t18-rodZ*].

For pCH395(D55A), a portion of pFB273(D55A) was amplified with primers 5'-GTACTCTAGAGGCCATTACGGCCATGAATACTGAAGCC-3' and 5'-CGGGATCCGGAGCTTTGCGGTCTTGCCACCACC-3'. The product was digested with *Xba*I and *BamH*I (underlined) and the 434 bp fragment was used to replace the 389 bp *Xba*I-*BamH*I fragment of pCH393 [P_{lac}::*t18-rodZ*(1-84)-*malF*(1-39)-*rfp*]. Other mutated versions of pCH395 were obtained similarly, using the corresponding mutated version of pFB273 (see below) as template.

Mutated versions of pFB273 [P_{lac}::*gfp-t-rodZ*] were generated by the Quickchange procedure (Stratagene), using mutagenic primers (altered bases underlined)
5'-GAAGATAAGGCACCCGCAGCGCTTGCTTCAACATTCCTG-3 (D55A),
5'-GATAAGGCACCCGCCGATGGCGCCTCAACATTCCTGCGCGG-3 (L56G),
5'-GCCGATCTTGCTTCAACAGCGCTGCGCGGATATATCCGC-3 (F60A),
5'-GCTTCAACATTCCTGCGCGGCGCCATCCGCTCTTATGCGCGTC-3 (Y64A),
5'-CATTCCTGCGCGGATATATCGCGTCTTATGCGCGTCTGGTAC-3 (R66A), or
5'-CCTGCGCGGATATATCCGCGCATATGCGCGTCTGGTACATATTCC-3 (S67A)
and their reverse complements. The entire *rodZ* ORF of each was sequenced to verify the presence of desired mutations, and the 508 bp *BamH*I-*Sal*I fragment of each mutant version was then used to replace the 262 bp *BamH*I-*Sal*I of pYT27 [*att*HK022 P_{lac}::*gfp-t-rodZ*(83-337)], yielding pFB273(D55A), pFB273(L56A), pFB273(F60A), pFB273(Y64A), pFB273(R66A), and pFB273(S67A).

The construction of pLP39 [*att*HK022 P_{lac}::*gfp-rodZ*(1-138)-*rfp*] involved several intermediate constructs. First, MG1655 chromosomal DNA was used as template to amplify the *mrcA* gene with primers 5'-GATCGGCCATTACGGCCGTGAAGTTCGTAAAGTATTTTTTG-3, and 5'-GATCGGCCGAGGCGGCCTCAGAACAATTCCTGTGCCTCGCC-3. The product was digested with *Sfi*I (underlined) and the 2566 bp fragment was

used to replace the 1027 bp *Sfi*I fragment of pCH371 [P_{lac}::*t18-rodZ*], yielding pLP7 [P_{lac}::*t18-mrcA*]. Second, oligos 5'-GATCGGCCATTACGGCCTAAGGCCGCCTCGGCC AG-3 and 5'-TCGACTGGCCGAGGCGGCCTTAGGCCGTAATGGCC-3 were annealed, yielding a 35 bp fragment with two internal *Sfi*I sites (underlined) that was used to replace the 1162 bp *BamH*I-*Sal*I fragment of pDR120 [P_{lac}::*gfp-ftsZ*], resulting in pLP13 [P_{lac}::*gfp-*]. Third, pLP14 [P_{lac}::*gfp-mrcA*] was obtained by replacing the 16 bp *Sfi*I fragment of pLP13 with the2565 bp *Sfi*I fragment of pLP7. Fourth, the 3364 bp *Xba*I-*Hind*III fragment of pLP14 was used to replace the 1115 bp *Xba*I-*Hind*III fragment of pTB183 [*att*HK022 P_{lac}::*gfp-zapA*], resulting in pLP20 [*att*HK022 P_{lac}::*gfp-mrcA*]. Finally, the 2566 bp *Sfi*I fragment of pLP20 was replaced with the 1153 bp *Sfi*I fragment of pCH395, giving rise to pLP39 [*att*HK022 P_{lac}::*gfp-rodZ*(1-138)-*rfp*]. Mutated versions of pLP39 were obtained as in the last step, but using the corresponding mutated version of pCH395 (see above) as source of the 1153 bp *Sfi*I fragment.